EUSIPCO 2013 1569742601

MULTI-CHANNEL PROCESSING FOR DIGITAL BEAM FORMING SAR

M. P. G. Otten, W. L. van Rossum, R. Tan, W. J. Vlothuizen, J. J. M. de Wit
TNO, The Hague, The Netherlands

ABSTRACT

A lightweight radar system, suitable for use on board small airborne platforms, has been built and tested. The radar system comprises a digital receive array, offering full beam forming flexibility at the cost of high data rates and heavy processing loads. In this paper, the requirements and architecture for multi-channel SAR processing are discussed and processing results from recent airborne campaigns are presented.

***Index Terms*—s**ynthetic aperture radar, digital beam forming, back projection, multi-channel processing

1. INTRODUCTION

The demand for light weight sensor suites for use on board small unmanned aerial vehicles (UAVs) is growing. In the field of radar, this has led to the use of frequency modulated continuous wave (FMCW) technology for light weight radar systems.

Most existing lightweight radars exploit conventional antenna technology. The radar system described in this paper applies Digital Beam Forming (DBF) on receive. DBF SAR will be part of a new generation of space-borne SAR systems [1], but for small airborne systems it has hardly been realized up to now. DBF has many operational advantages, a few of which are the following:

- In conventional Synthetic Aperture Radar (SAR) there is a fundamental trade-off between coverage and resolution (i.e. Strip SAR or Spot SAR). With DBF multiple high-gain receive beams can be formed, which allows much wider coverage with high resolution, limited mainly by processor capacity.
- Wide-beam illumination and multiple receive channels allows advanced Ground Moving Target Indication (GMTI) modes, using Space Time Adaptive Processing and high update rates for slow moving target detection and fast target tracking.
- In Coherent Change Detection the coherence is maximized by the possibility to steer the (receive) beams optimally, by selecting the best beam directions after the second pass.

To benefit from these advantages, high data rates and heavy processing loads must be supported. At the same time, the application in tactical UAVs demands low volume and power for both sensor and processor.

This paper describes the processing requirements and algorithms and the multi-channel processing architecture.

2. DESCRIPTION OF THE AMBER RADAR SYSTEM

The design [2], [3] of AMBER (Affordable Multi-BEam Radar) was driven by the requirement of 10 cm resolution, and ranges up to 5 km. The system features a wide beam transmitter and 24 digitized receive channels, sampled at 20 MHz each. To keep the beat frequencies to be sampled sufficiently low, long sweeps are used in the SAR modes to enable use of the full 1.5 GHz signal bandwidth. In GMTI modes, higher sweep repetition frequencies are applied, but with lower signal bandwidth. The AMBER hardware is shown in Figure 1.

Figure 1. The AMBER radar hardware, including data storage on solid-state disks.

One of the novel SAR modes is simultaneous Strip and Spot SAR [4]: a conventional single beam SAR system can have either a fixed antenna beam (i.e. Strip SAR with medium resolution), or a steered beam (i.e. Spot SAR with high resolution). With AMBER these modes can be performed simultaneously, see Figure 2, where the main practical limitation is determined by processing capacity. Another novel SAR mode is the wide-beam SAR mode, see Figure 3, where a large area is imaged from only a short data take, i.e. just long enough to achieve the required resolution (seconds). This has several advantages; it reduces the amount of required motion compensation (since the track is short) and operationally it makes the radar much harder to detect (i.e. Low Probability of Intercept), since it only has to transmit for a few seconds, instead of transmitting continuously. All the above advantages depend on the ability of the processor to handle multiple-beam SAR imaging; the challenge is on the processor.

3. PROCESSING REQUIREMENTS

3.1. Algorithms

Over the last years the interest in special processing for FMCW SAR has increased. Many adapted processing techniques are based on conventional algorithms such as the

range-Doppler or ω–k algorithms, e.g. [5]. For the current system, however, multi-channel Back Projection processing in time domain is foreseen [6]. Efficient frequency domain algorithms are inherently less flexible, as they require block-oriented (FFT) processing structures, and most of these algorithms are limited when it comes to wide-band and wide-angle processing, often requiring approximations which become invalid under wide-band/wide-angle conditions. The time domain approach does not have any of these disadvantages, but requires a number of computations that may be several orders of magnitude higher. Back Projection has been applied before to SAR in low-frequency SAR and bistatic SAR [7], [8]. In the case of AMBER, another dimension to the back-projection is added, which is formed by the 24 receive channels.

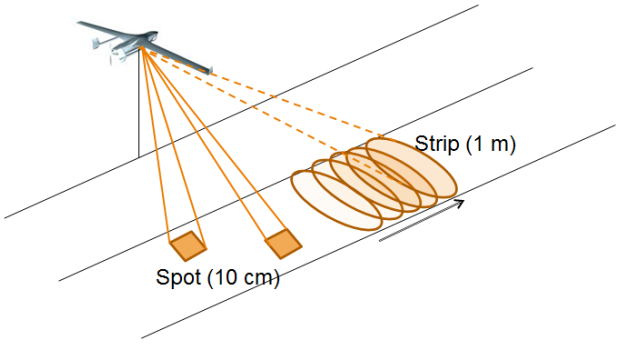

Figure 2. Simultaneous Strip and Spot SAR modes.

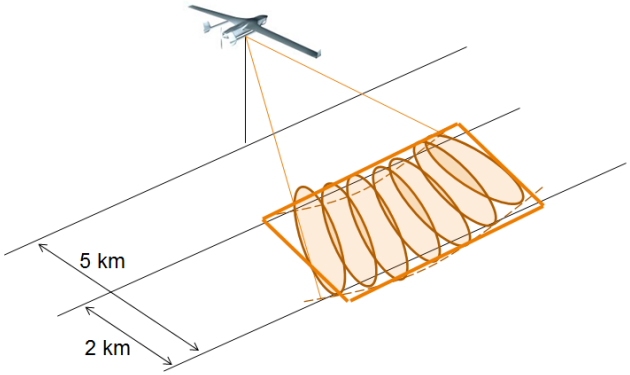

Figure 3. Wide-beam SAR mode.

The AMBER sensor is an FMCW radar system. The received signal is mixed with the transmitted signal, which yields beat signal. For a single target the received signal as function of fast time, t is given as:

$$s_n(t) = A \cdot \exp\left(i \cdot 2 \cdot \pi \cdot \left[\left\{f_{start} + \gamma \cdot t\right\} \cdot \tau_n + \tfrac{1}{2} \cdot \gamma \cdot \tau_n^2\right]\right).$$

Here, the subscript n indicates the n^{th} sweep, A the complex amplitude of the signal, incorporating the radar equation, f_{start} the start frequency of the waveform and γ the chirp rate (the transmitted bandwidth, B divided by the sweep time, T_{sweep}). The time delay between the transmitted signal and the received signal scattered by the target at range R_n is given as:

$$\tau_n = \frac{2R_n}{c}.$$

Here, c is the speed of light in air. For a moving target the distance changes constantly which results in a change of the time delay and therefore the phase (this is known as the Doppler frequency). For a stationary target but with a moving platform the distance, and therefore the time-delay and phase, also changes constantly.

The SAR processor sums coherently the response which corresponds to a single grid/target position at (x,y,z). The signal after compression becomes:

$$s(x,y,z) = \sum_t \sum_n s_n(t) \cdot \exp\left(-i \cdot 2 \cdot \pi \cdot \left[\left\{f_{start} + \gamma \cdot t\right\} \cdot \tau_n + \tfrac{1}{2} \cdot \gamma \cdot \tau_n^2\right]\right).$$

Targets at different positions (in range and/or azimuth) have different phase behaviors as function of fast time t and/or slow time index n, and therefore result in responses at different positions (x,y,z).

For AMBER, the signals at the different receive elements of the array can be treated as independent measurements and the sum can be extended to include the different elements:

$$s = \sum_m \sum_t \sum_n s_{n,m}(t) \cdot \exp\left(-i \cdot 2 \cdot \pi \cdot \left[\left\{f_{start} + \gamma \cdot t\right\} \cdot \tau_{n,m} + \tfrac{1}{2} \cdot \gamma \cdot \tau_{n,m}^2\right]\right).$$

Here, m indicates the different receive channels. The triple sum above can be compared with classical 2D beam forming (sum over m), pulse compression (sum over t) and azimuth compression (sum over n). The time delays are functions of the position of the antenna element and the target/grid position:

$$\tau_{n,m}(x,y) = \frac{2 \cdot R_{n,m}}{c} = \frac{2}{c} \cdot \sqrt{\left(x_{n,m} - x\right)^2 + \left(y_{n,m} - y\right)^2 + \left(z_{n,m} - z\right)^2}.$$

While Back Projection processing is massive, current hardware solutions can handle the required amount of computation. For instance, various GPU based solutions have been proposed and implemented [9].

For the AMBER system the processing steps are shown in Figure 4. Back Projection in this case can operate over three sampling domains: 1) receive elements, 2) fast-time samples (one transmitted sweep), and 3) slow-time samples (aircraft positions along the track); the latter creates the synthetic aperture to achieve high cross range resolution. Traditionally, antenna elements are added directly at RF level to form a single beam in a desired direction, but adding the channels digitally as part of the overall Back Projection sum allows better image quality when the processed angles

are wide; for narrow angles, an independent DBF summation is sufficient. In the fast-time domain, there is little advantage in time domain processing, so that here, the faster frequency domain processing is still preferred (i.e. the range FFT).

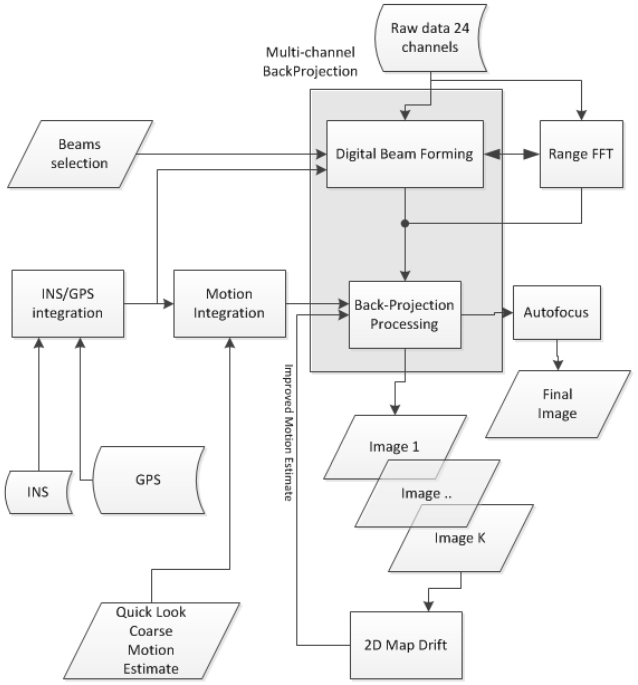

Figure 4. DBF SAR processing chain.

After a data decimation step, the DBF is controlled by the radar operational mode and by the platform attitude (yaw and pitch). Range resolution is achieved by FFT processing of the transmitted waveform, and cross range resolution is achieved by coherent integration along the flight path. The Back Projection is carried out in time domain onto a 3D surface (earth) and constitutes the heaviest processing load. Furthermore, since navigation sensors alone (inertial sensors and GPS) are not accurate enough (mm accuracy is required!), several stages of iterative autofocus are necessary. First Map Drift (or subaperture) processing is applied to compensate the relatively large errors and subsequently the Phase Gradient Algorithm (PGA) [10] is used to compensate the residual motion errors (i.e. the "Autofocus" block).

3.2. Real-Time requirements

The AMBER system front-end delivers 24 channels sampled at 20 MHz with 12 bit per samples. This represents a data rate of 5.8 Gbit/s. These data are currently filtered and down sampled by a factor of two, and then distributed to 3 (or up to a maximum of 6) solid-state disks, and streamed to the SAR processor. The decimation and data handling is performed by an FPGA inside the radar unit. Another decimation step may be performed by the SAR processor depending on the selected radar mode.

The amount of computation varies per radar mode. One of the most demanding modes is the Spot SAR mode. For a Spot SAR mode with a single beam and a 500 m by 500 m image with 10 cm resolution, the estimated load is given in Table I.

Table I. The estimated processing load for the Spot SAR mode.

Operation	**Gflops/s**	
Decimation-I/Q	2	24 channels
Beam Forming	0.1	Per SPOT area
Range FFT	0.3	
Azimuth Back Projection	75	

The computational load for autofocus is very dependent on the initial navigation data quality and the platform motion. However, assuming several iterations of Map Drift processing[1], and some fine tuning with PGA, it is clear that the processing load is several hundred Gflops, where the main load is in the Back Projection step. If we want to process multiple SPOT areas simultaneously, which is possible thanks to DBF, this amount is multiplied accordingly. As it is quite easy to specify a multi-area high resolution mode that cannot be processed in any (current) limited size processor, the processor capacity will drive the operational capabilities of the system.

4. PROCESSING RESULTS

In this section some of the processing results are presented obtained during two measurement campaigns in spring and autumn of 2012. All images shown here were processed off-line. More recent flight and processing results will be presented later.

4.1. Measurement campaigns

In April 2012 the AMBER system was successfully demonstrated for the first time on a helicopter test flight above the city of Naarden in The Netherlands, see Figure 5. During the flight a number of radar recordings were made using different SAR modes, which were processed off-line afterwards. Some of the resulting SAR images are presented in Section 4.2.

After the test flight of Spring 2012, the bandwidth of the AMBER system was increased to 1 GHz, enabling a range resolution of 0.15 m. Also, the system was prepared for its second flight to be carried out in the autumn of 2012. This meant making the system flight certified to be carried in a pod under the wing of the Stemme S15 motor glider (see Figure 6). The second test flight was carried out in October 2012 near the town of Marnehuizen in the north of

[1] re-focusing can be carried out faster than initial focusing

the Netherlands. Radar data were collected using both SAR and GMTI modes. Some of the GMTI results are presented in Section 4.3. In May 2013 a third test flight has been organized to show AMBER's high resolution capabilities.

Figure 6. AMBER installed in the under wing pod of the Stemme S15 motor glider during the second test flight in Marnehuizen.

4.2. Synthetic aperture radar results

In Figure 7 a SAR image of Naarden in The Netherlands is shown using the wide-beam SAR mode described in Section 2. The image was made from three seconds of radar data (signal bandwidth 300 MHz; sweep repetition frequency 312 Hz). Using DBF, many different beams were combined to form the total wide-area image covering several square kilometer. The final image has a resolution of approximately 0.5 m. In the May 2013 campaign, 15 cm resolution was demonstrated. In Figure 8 a detail of the total image is shown, revealing parked cars at the edge of the city center.

4.3. Ground moving target indication results

The results obtained with the GMTI mode are shown in Figures 9 and 10. Figure 9 shows a radar image made with a narrow beam using DBF with all 24 channels. In this image two cars have been detected moving away from the radar, (the blue circles) and three cars have been detected moving toward the radar (the red circles). The cars appear at the correct range in the image (horizontal), but at incorrect azimuth (vertical) due to their speed.

Using the antenna array of AMBER, the correct azimuth angle to the target can be estimated from the data making it possible to place the detected cars back at the correct position in the image. Furthermore, since the measurement geometry is known, the ground speed of the cars can also be estimated. This has been done in Figure 10. The background image is a wide-beam SAR image of the area around Marnehuizen. The red and blue circles are now at the actual positions of the detected cars. Also, the estimated velocities of the cars are indicated. The number of cars detected and their direction of motion correspond with the ground truth provided by camera imagery. Note that the cars are on a regional road with a speed limit of 80 km/h, such that the estimated velocities seem plausible.

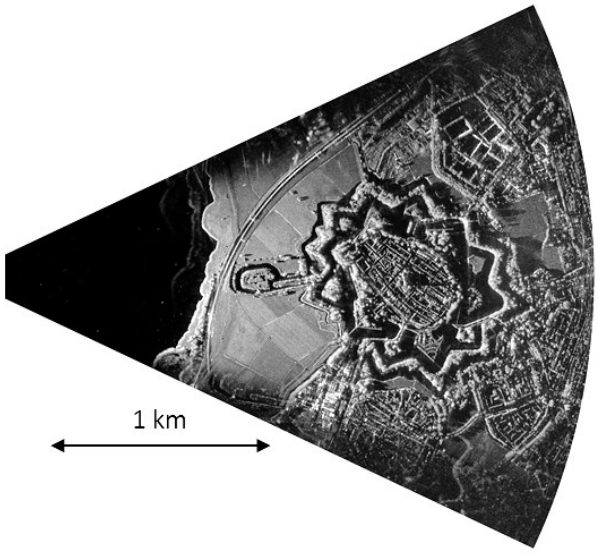

Figure 7. A Wide-beam SAR image of Naarden covering several square kilometer and a resolution of 0.5 m. This image has been constructed by combining 120 different beams using DBF. This image was formed from three seconds of data, while a conventional strip mapping SAR on a slow-flying UAV would have required almost two minutes to scan the area. The characteristic star-shape is outlined by the walls of an old historic fortification and a moat (dark parts).

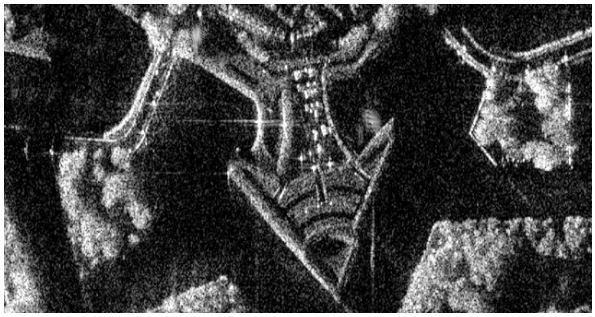

Figure 8. Detail of the Wide-beam SAR image showing parking spaces and parked cars at the edge of the Naarden town center.

5. PROCESSING ARCHITECTURE

Based on the predicted processing load and tests performed with Back Projection we propose a flexible processing architecture based on FPGA, CPU and GPU elements. The CPU and GPU are located in a small processing cabinet which connects to the FPGA that control the AMBER radar via a 10 Gbps optical link.

The processing steps of Figure 4 are mapped to these resources. Decimation/IQ demodulation is mapped to the FPGA, because of its regular structure which suits the FPGA programming model, and because of the data reduction. Beam forming in its simplest form is also suitable for FPGA implementation, and leads to data reduction unless many beams are formed. If adaptive beam forming is

required or many beams are required, beam forming can also be done on the GPU or even the CPU.

Back Projection requires significant processing power and is very well suited to implementation on a GPU because it can be parallelized quite well. GPUs nowadays are faster at FFT processing than CPUs, but the CPU will probably have more than enough computing power to perform the range FFT. The choice will therefore depend on practical concerns of data locality. All other processing steps will be performed on the CPU. The CPU will also perform the coordination of the data flows between the various resources. This architecture is being set-up and real-time processing of AMBER data will be demonstrated in the course of 2013.

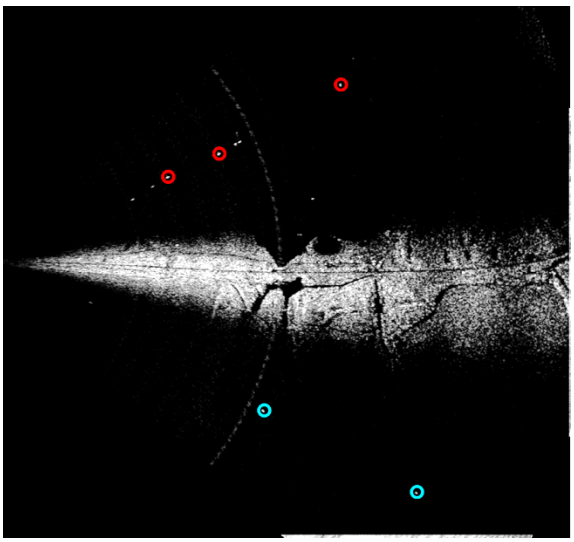

Figure 9. GMTI radar image of Marnehuizen made with 24 channels. Three cars moving away from the radar (red circles) and two cars moving towards the radar (blue circles) have been detected.

6. CONCLUSIONS

A compact multi-channel SAR has been presented; in this novel type of SAR, the capability of the sensor is inherently large, allowing many new (simultaneous) SAR and GMTI modes, but the capability system as a whole is largely dependent on the processing capacity, which has to be realized in a relatively small volume, weight and power, in order to be compatible with small airborne platforms, such as a tactical UAV.

Multi-channel SAR processing has been demonstrated off-line with flight tests, showing novel wide-beam SAR modes and GMTI modes. The computational load for high resolution SAR imaging is in the order a several hundred Gflops, which is mostly due to the Back Projection algorithm. A real-time processor architecture is being set-up, consisting of FPGA, CPU and GPU processing elements, where the most demanding computation step is performed on GPU. With this processor real-time processing of AMBER data will be demonstrated in 2013.

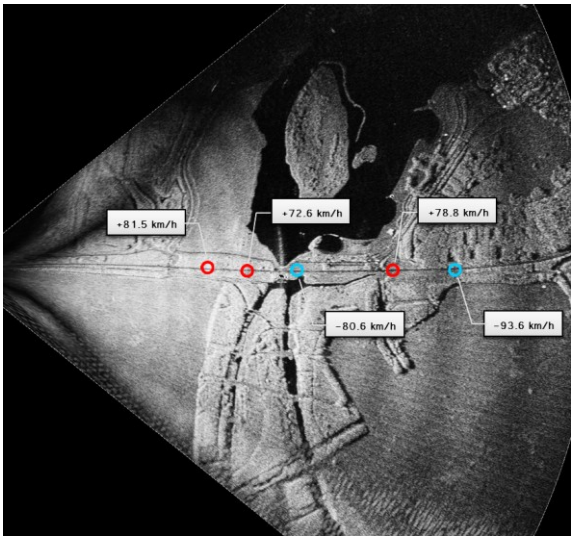

Figure 10. Ground moving target indication results. Using the antenna array of AMBER the correct azimuth angle of the cars from Figure 9 has been estimated. Also the ground speed of the cars has been estimated. The background is a wide-beam SAR image of the area around Marnehuizen.

7. REFERENCES

[1] S. Huber, M. Younis, A. Patyuchenko, G. Krieger, “A novel digital beam-forming concept for spaceborne reflector SAR Systems” in Proc. EuRAD, Rome, Italy, 2009.

[2] M. P. G. Otten, A. P. M. Maas, R. J. Bolt, and L. Anitori, “Light Weight Digital Array SAR,” in Proc. IEEE Phased Array, Boston, U.S.A., Oct. 12-15, 2010, pp. 177-182.

[3] W. L. van Rossum, M. P. G. Otten, and Ph. van Dorp, “Multichannel FMCW SAR,” in Proc. EUSAR, Nuremberg, Germany, April 23-26, 2012, pp. 279-282.

[4] J. J. M. de Wit, “Innovative SAR/MTI concepts for digital radar,” in Proc. EUSAR, Friedrichshafen, Germany, June 2-5, 2008, pp. 89-92.

[5] J. J. M. de Wit, A. Meta, and P. Hoogeboom, “Modified range-Doppler processing for FM-CW synthetic aperture radar,” IEEE GRSL, vol. 3, no. 1, pp. 83-87, 2006.

[6] W. J. Vlothuizen and M. Ditzel, “Real-time brute force SAR processing,” in Proc. IEEE Radar Conf., Pasadena, U.S.A., May 4-8, 2009.

[7] L. M. H. Ulander, H. Hellsten, G. Stenstrom, “Synthetic-Aperture Radar Processing Using Fast Factorized Back-Projection,” IEEE Trans. AES, vol 39, no. 3, July 2003.

[8] L. M. H. Ulander, P.-O. Frölind, A. Gustavsson, D. Murdin, and G. Stenström, “Fast factorized back-projection for bistatic SAR processing,” in Proc. EUSAR, Aachen, Germany, June 2010.

[9] B. Liu, K. Wang, X. Liu, and W. Yu, "An Efficient Signal Processor of Synthetic Aperture Radar Based on GPU," in Proc. EUSAR, Aachen, Germany, June 2010.

[10] T. M. Calloway, C. V. Jakowatz, F. A. Thompson, and P. H. Eichel, "Comparison of synthetic aperture radar autofocus techniques; phase gradient vs. subaperture," in Proc. SPIE Advanced Signal Process. Algorithms, Architectures, and Implementations II, Bellingham, U.S.A., July 1991.